NANO LETTERS

Letter

pubs.acs.org/NanoLett

Direct Observation of Ordered Configurations of Hydrogen Adatoms on Graphene

Chenfang Lin,[†] Yexin Feng,*[,‡,§] Yingdong Xiao,[†] Michael Dürr,[∥] Xiangqian Huang,[†] Xiaozhi Xu,[†] Ruguang Zhao,[†] Enge Wang,*[,‡,§] Xin-Zheng Li,[†,‡] and Zonghai Hu*[,†,‡]

[†]State Key Lab for Mesoscopic Physics, School of Physics, Peking University, Beijing 100871, China

[‡]Collaborative Innovation Center for Quantum Matter, Beijing, China

[§]International Center for Quantum Materials, School of Physics, Peking University, Beijing 100871, China

[∥]Institute of Applied Physics, Justus Liebig University Giessen, 35392 Giessen, Germany

Supporting Information

ABSTRACT: Ordered configurations of hydrogen adatoms on graphene have long been proposed, calculated, and searched for. Here, we report direct observation of several ordered configurations of H adatoms on graphene by scanning tunneling microscopy. On the top side of the graphene plane, H atoms in the configurations appear to stick to carbon atoms in the same sublattice. Scanning tunneling spectroscopy measurements revealed a substantial gap in the local density of states in H-contained regions as well as in-gap states below the conduction band due to the incompleteness of H ordering. These findings can be well explained by density functional theory calculations based on double-sided H configurations. In addition, factors that may influence H ordering are discussed.

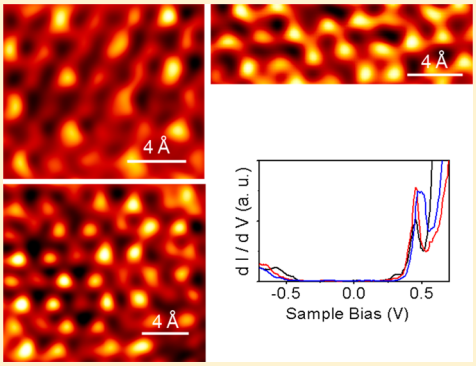

KEYWORDS: *Graphene, hydrogen, ordered, double-sided, STM, gap*

Adsorbates can vastly change the atomic and electronic structures of two-dimensional (2D) materials. Therefore, they are major candidates for property tuning and producing new materials especially if they form ordered configurations.[1−4] Hydrogen/graphene has become a model system because graphene is the most studied 2D material and hydrogen is the simplest adsorbate species. This system also finds practical relevance in hydrogen storage,[5] H_2 formation in the universe,[6] Tokamak wall erosion,[7] and recently, graphene based electronic and spintronic devices.[8−11] Concerning this most recent development, ordered configurations have received great attention because they are closely tied to tuning of graphene properties including large band gap opening and formation of specific magnetic orders, both of which are highly desirable in potential applications. Hydrogenation can induce magnetic moment, enhance the spin−orbit coupling and change the magnetic properties of graphene.[12−15] An imbalance in the H occupancy of the two sublattices can generate ferromagnetism in graphene. Ordered H distributions rather than random ones are better for realizing this imbalance. Pristine graphene is a zero gap semiconductor with exotic properties.[16,17] However, a band gap is needed in devices such as field effect transistors. Hydrogenation has emerged as a promising method to generate an energy gap in graphene.[1,2,8−11,18,19] Elias et al. demonstrated a disorder-induced metal−insulator transition and a mobility gap after hydrogenation of graphene on SiO_2 substrates.[2,18] After double-sided hydrogenation of suspended graphene, they observed structural deformation in the carbon lattice, a sign of graphane-like structures.[1,2] Balog et al. studied the case of patterned hydrogen adsorption on graphene moiré superstructures on Ir(111). They proposed a graphane-like ordered structure in the hydrogenated area involving C−Ir bonding to explain the coverage-dependent energy gap as a confinement effect.[8,9] To achieve practical on/off performance in devices at room temperature, a true band gap is highly beneficial. This requires that the H adatoms should be in ordered configurations.

Many ordered structures of hydrogenated graphene have been proposed, including double-sided and single-sided ones, with the calculated band gap width depending on the respective H coverage.[1,8,20−22] For example, theoretical work by Sofo et al. showed that graphane, the fully hydrogenated graphene monolayer with the H atoms bonding to carbon on both sides of the plane in an alternating manner, possesses a band gap larger than 3.5 eV.[1] However, although these ordered structures have received broad attention, none has been observed directly and the possibility of ordered hydrogenation of graphene remains in doubt to date. To the contrary, pairing

Received: September 22, 2014
Revised: January 3, 2015
Published: January 26, 2015

DOI: 10.1021/nl503635x
Nano Lett. 2015, 15, 903−908

and clustering of H adatoms have been observed in single-sided hydrogenation, and the H atoms appear to be disordered.[23−27]

To lift the above uncertainty, here we report direct imaging of several ordered configurations of H adatoms on graphene by scanning tunneling microscopy (STM). The H atoms in the configurations exhibit apparent sublattice selectivity and tiny deviations from the exact atop-of-carbon positions. In relatively ordered H-containing regions, scanning tunneling spectroscopy (STS) measurements showed a gap larger than 0.6 eV in the local density of states (LDOS) as well as in-gap states due to disorder (incomplete H ordering). These findings can be well explained by our density functional theory (DFT) simulations based on models of double-sided H configurations. Factors that may influence H ordering are also discussed.

Results and Discussion. Graphene samples grown on copper foil by the standard chemical vapor deposition (CVD) method[28,29] were dosed with a hydrogen beam generated in a hot capillary heated to >2900 K. The typical H dosage was at a flux of $\sim 1 \times 10^{11}$ cm^{-2}/s for 2 h. STM was done in UHV at 77K. DFT calculations were performed using the VASP code with the Perdew−Burke−Ernzerhof (PBE) functionals.[30,31] The projector augmented wave (PAW) potentials were used with a 700 eV plane wave cutoff energy. Binding energies of configuration A, B, and C were calculated employing a 6×6 graphene supercell with a $3 \times 3 \times 1$ mesh of the Monkhorst−Pack k points. The H diffusion barriers were calculated using the climbing image nudged elastic band (NEB) method.[32]

Figure 1 shows the Raman spectra of the samples. The intensity of the defect-associated graphene D band (I_D) increases with the H dosage, indicating H uptake. Meanwhile the G band broadens and the D′ band emerges. From the I_D/I_G ratio, the H coverage of the sample corresponding to the blue spectrum is estimated to be 4%.[33] We note that the H coverage is not uniform over the surface. Some areas appear clean of H while others have high H coverage.

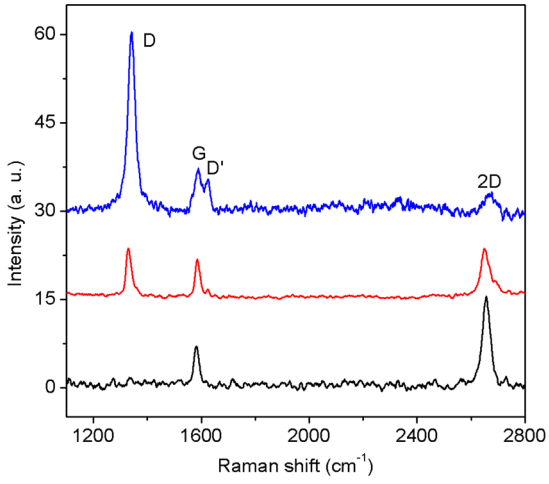

Figure 1. Raman spectra of as-grown graphene (black), graphene exposed to a lower H dosage (red), and a higher dosage (blue) with an excitation wavelength of 633 nm. The intensity is renormalized to the G band intensity. The background caused by the substrate was subtracted and the spectra were vertically displaced for clarity. The increase of I_D and I_D/I_G ratio with increasing H dosage indicates H uptake.

Atomically resolved STM images of some ordered H configurations and their corresponding schematic diagrams are shown in Figure 2. H adatoms appear as the bright spots in STM. Configuration A in Figure 2a exhibits a $\sqrt{3} \times \sqrt{3}$/R30° structure with respect to the graphene lattice (for convenience we call this configuration "graphine"). A closer look at Figure 2a reveals that the H atoms appear a little bit off the "on-top" positions of the occupied carbon sites, upward along the C−C bonds. Configuration B in Figure 2c can be viewed as two staggered sets of "graphine", displaced by a lattice constant of graphene. However, there is a subtle deformation of the hexagonal shape as illustrated in Figure 2d, $|AB| \times 2 > |CD|$. Configuration C in Figure 2e can be considered as three interleaving sets of "graphine", displaced to each other by the lattice constant (every other carbon site appearing bright). In our experiments, configurations B and C were more often observed than configuration A. Extended area larger than a few nm^2 of one single configuration was hard to obtain. Instead, mixture of the three configurations and missing of H atoms were often seen, as shown in Figure 2g,h. Interestingly, almost all the bright spots appear to occupy the same sublattice. Though it seems that some of the graphene honeycomb cells are deformed and the H ordering is far from perfect, significant ordering is still found in the corresponding fast Fourier transformation (FFT) shown in Figure 2i. The diffraction spots marked by the blue circles correspond to the graphene lattice and configuration C. Spots in the white circles correspond to configurations A and B (containing the $\sqrt{3} \times \sqrt{3}$/R30° structure).

The STM tip could disturb the configurations from time to time, especially with large values of bias and tunneling current. Figure 3a,b shows STM scans of the same area with a time interval of 10 min. The white circles highlight one of the disappearing bright spots in the later scan. Notably, this verifies that the bright spots seen here are indeed H adatoms, not the scattering patterns caused by nearby defects.[34]

To investigate the effects of these ordered H configurations on the electronic structure of graphene, STS measurements were taken and significant changes in the LDOS were observed. Figure 3d,e shows typical STS results. There is a gap in the LDOS (0.6 eV in Figure 3d and 1.2 eV in Figure 3e). As a comparison, STS results of clean graphene regions (Figure 3c) show the well-known Dirac point feature. There is another interesting feature in Figure 3d,e, the small peak just below the conduction band. The origin of this feature will be explained later on.

Extensive studies have shown that the single-sided meta-dimers (H occupying two next-nearest-neighbor sites in one hexagon) are energetically much less stable than the ortho-dimers (two nearest-neighbor sites) and para-dimers (two sites on the opposite corners of one hexagon),[23] so is the chair-graphone configuration (H atoms fully occupying one sublattice).[35] Therefore, by first sight our observation of the ordered H atoms (bright spots) occupying the same sublattice is puzzling. However, since graphene is only weakly bounded to the Cu substrate and intercalation can happen,[36−39] another possible scenario is that the bright spots correspond to double-sided ortho-dimers (one H above and one below the graphene plane on two nearest neighbor sites) and only the top-sided H atoms are seen in STM. To check the validity of this assumption, we carried out DFT calculations. Good agreements with our experimental results were found. The binding energies per H atom for several structures on freestanding monolayer graphene are summarized in Table 1. Indeed, our calculations show that the double-sided ortho-dimer is the most stable

DOI: 10.1021/nl503635x
Nano Lett. 2015, 15, 903−908

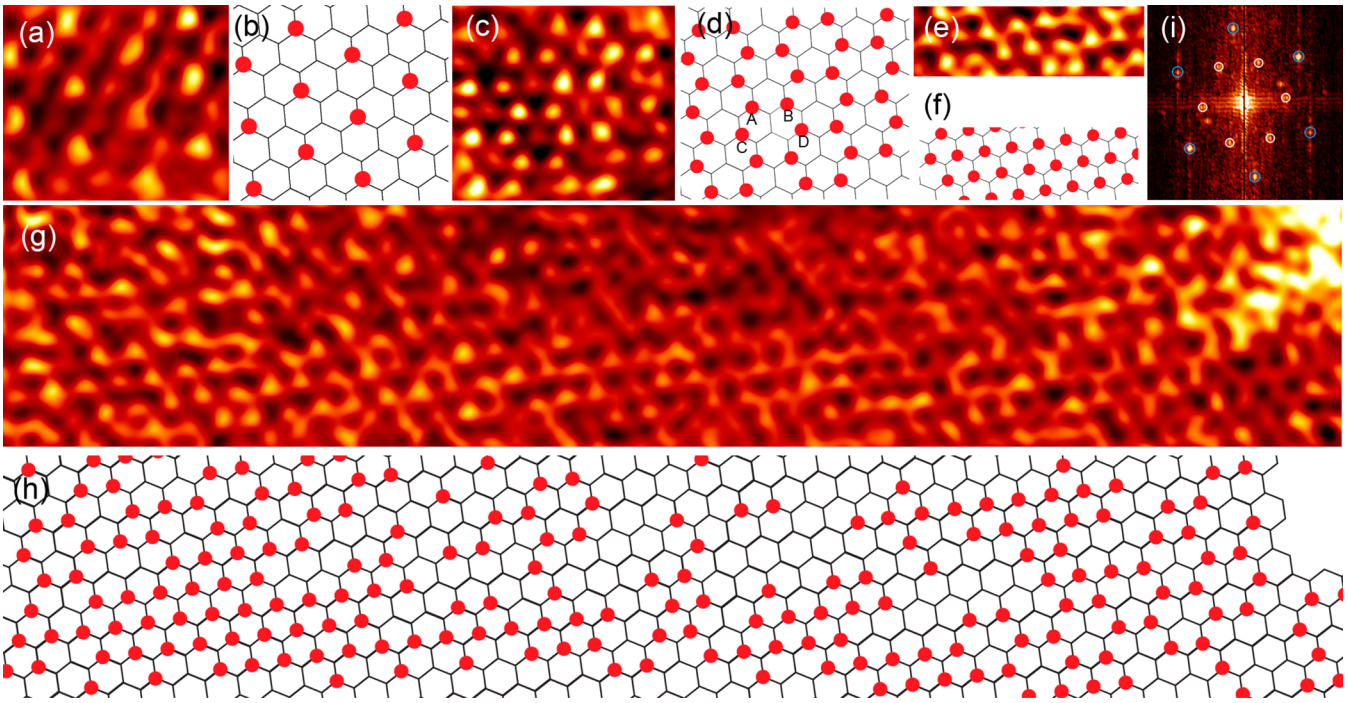

Figure 2. STM images showing ordered configurations of H adatoms. (a,b) Configuration A (graphine). The H atoms appear a little bit off the "on-top" positions of the occupied carbon sites, moving upward along the C−C bonds. (1.4 nm × 1.2 nm scan size). (c,d) Configuration B. |AB| × 2 > | CD|. (1.8 nm × 1.6 nm); (e,f) Configuration C. (1.9 nm × 0.6 nm). (g,h) Mixing of the three structures mentioned above. (i) Fast Fourier transformation of panel g. The spots corresponding to the graphene lattice and the $\sqrt{3} \times \sqrt{3}$/R30° hydrogen structure are marked by the blue and white circles, respectively. Scanning conditions: tunneling current 0.1 nA, sample bias −1 V.

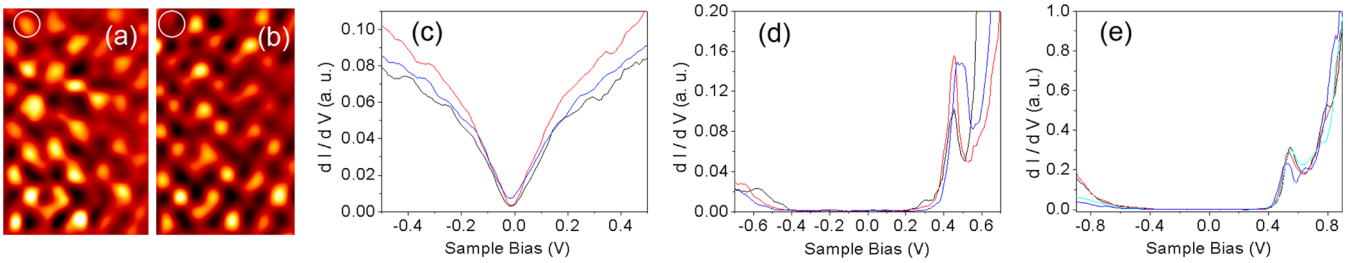

Figure 3. (a,b) Consecutive STM scans of the same area. The white circles highlight one of the disappearing H atoms. (c)STS results taken at different points in clean regions (without H atoms), showing the Dirac point. (d,e) Typical STS results in H-containing regions corresponding to Figure S2 in the Supporting Information and Figure 2g, respectively, showing the usually observed gap width ranging from 0.6 to 1.2 eV in the LDOS. Set point: I = 0.2 nA, sample bias V = −1 V, modulation voltage (peak-to-peak value) ΔV = 10 mV.

Table 1. H Binding Energies Per H Atom for Several Structures[a]

structure	monomer	d-ortho	d-para	d-meta	s-ortho	s-para	s-meta	s-A	d-A	d-B	d-C
E_b (eV)	0.83	1.66	1.27	0.76	1.38	1.35	0.76	0.76	1.82	2.22	2.45

[a]"s" denotes single-sided and "d" denotes double-sided. "ortho", "para", and "meta" denote the different dimer configurations. A, B, and C stand for the ordered structures observed in our STM experiments.

dimer configuration, which is in agreement with recent reports.[40] For configuration A, we first considered single-side hydrogenation (denoted as s-A in Table 1) with H coverage of 1/6. The resultant H binding energy is even lower than that of isolated H monomers. This indicates that although the single-sided model will give the look of configuration A, it is energetically unfavorable. For configuration A with double-sided ortho-dimers (denoted as d-A in Table 1), the resultant H binding energy is much higher than all isolated dimer configurations. The binding energies of double-sided configurations B and C are even higher. This indicates that all the three double-sided configurations are energetically more favorable than isolated H monomers or dimers.

Figure 4 shows the 2D partial charge density distributions of double-sided configurations A, B, and C together with the atomic structures. A close look at Figure 4a reveals that because of the existence of the bottom-sided H atoms at the nearest neighbor carbon sites, the top-sided H atoms (the bright spots) appear to move toward the center of the C−C bonds, in contrast to the on-top positions of H monomers. Such a phenomenon is indeed observed in Figure 2a as mentioned above. Moreover, Figure 4b reveals that similar small deviations from the on-top positions lead to apparent distortion of the

DOI: 10.1021/nl503635x
Nano Lett. 2015, 15, 903−908

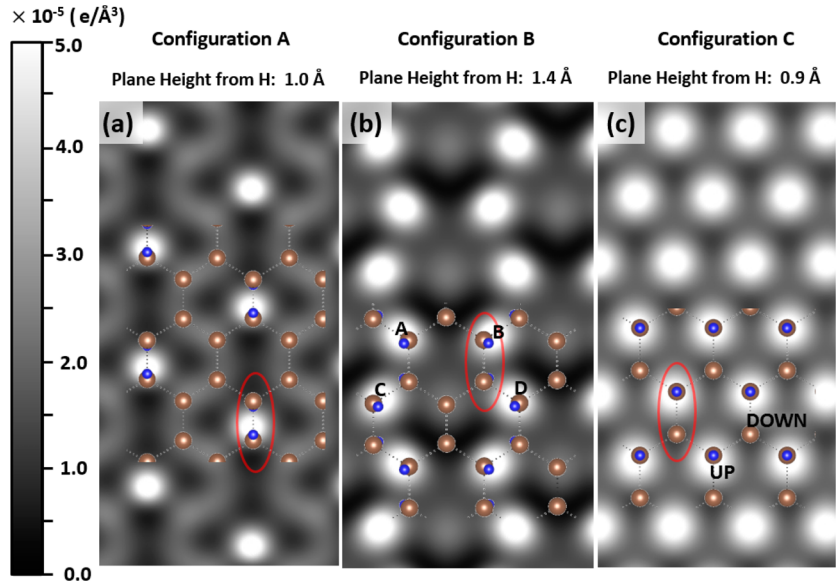

Figure 4. DFT simulation results of the 2D contours of the electron partial charge density for configurations A, B and C. The brown (blue) balls mark the C (H) atoms. The double-sided ortho-dimer units are indicated by the red ovals. (a) The H atoms appear a little bit off the "on-top" positions of the occupied carbon sites, moving upward along the C−C bonds. (b) |AB| × 2 > |CD|.

hexagonal shape of the bright spots, so that |AB| × 2 > |CD|, again in excellent agreement with the STM image Figure 2c. These detailed agreements further support the double-sided picture of the ordered H configurations.

Figure 5 shows the band structures and DOS for the three configurations ideally ordered and extended. A gap exists in all of them. Configuration A possesses a gap of 0.6 eV, while both configurations B and C have a wide clean band gap larger than 3.4 eV. Our typical STS results showed gaps ranging from 0.6 to 1.2 eV in the LDOS. However, there is a small peak below the conduction band and no gap much larger was observed. To explain these results, we first note that the H-contained regions in our samples are similar to those shown in Figure 2g and Supporting Information Figures S1 and S2, far more disordered than the idealized structures shown in Figure 2a−f. To simulate this disorder effect in DFT calculations, we introduced some H vacancies in a graphane sheet (configuration C) and considered four random models as shown in Figure 6. The corresponding DOS shows dependence on the H coverage (degree of disorder). Moreover, defect states (small peaks as marked by the blue arrows) appear in the gap between the valence band maximum (VBM) and the conduction band minimum (CBM), which are marked by the red arrows. As the disorder increases (the H coverage decreases), these defect states gradually merge with the VBM/CBM. The effective energy gap gets smaller and smaller, for example, to about 0.4 eV as in the case shown in Figure 6d. This disorder effect on the electronic structure explains why the gap width usually observed in our STS measurements is about 0.6−1.2 eV, not much larger. Meanwhile, the characteristic peak below the CBM in our STS curves is also reflected in Figure 6c,d. This study demonstrates that to obtain a relatively clean band gap, formation of highly ordered hydrogen areas is needed. Some factors that may influence H ordering are discussed below.

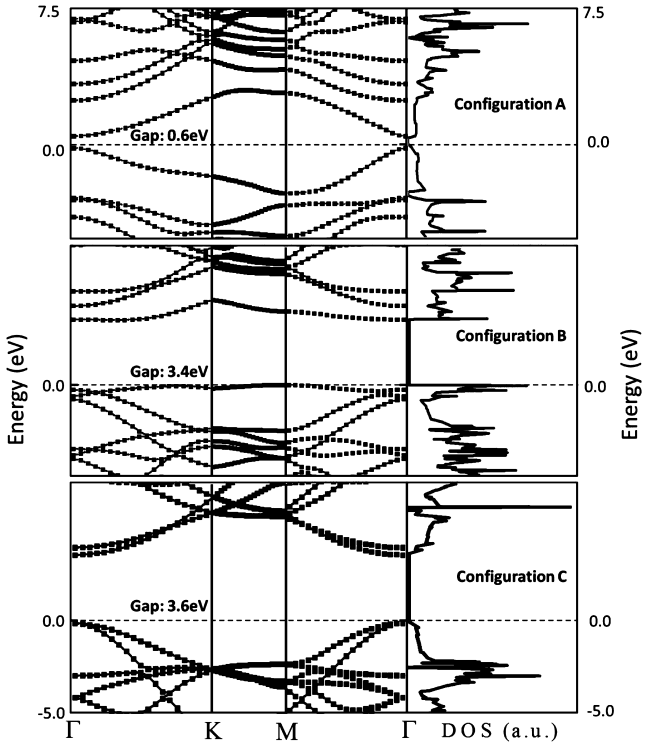

Figure 5. DFT results of the band structures and DOS for perfect configurations A, B and C.

Because of the sublattice compatibility on each side of the graphene plane, all three configurations can be considered as partial formation en route to a complete chair graphane structure that has the highest binding energy per H atom among all configurations. Besides the binding energy, there are various dynamic processes including adsorption, diffusion, abstraction, and desorption that can affect H ordering.[3,7,41−43] Because the kinetic energy of the H atoms generated in our hot capillary (>2900 K) is higher than the reported ∼0.2 eV adsorption barrier on clean graphene surface,[24,44] the sticking sites should be largely random. Therefore, adequate H diffusion should be important for ordering. H atoms can find energetically favorable positions through diffusion. Because H is the lightest atom, quantum treatment of the proton

DOI: 10.1021/nl503635x
Nano Lett. 2015, 15, 903−908

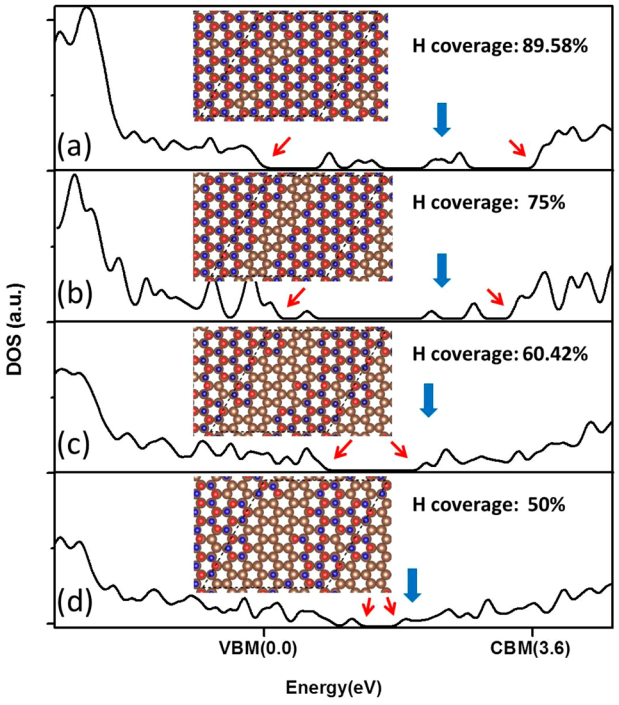

Figure 6. DOS curves of hydrogenated graphene sheets with different levels of disorder (H coverage) from DFT simulations are illustrated. The corresponding atomic structures are also presented. The brown balls represent C atoms and the red/blue balls represent H adatoms above/below the graphene sheet. The blue arrows mark the in-gap states. The red arrows mark the positions of VBM/CBM. The positions of VBM/CBM for configuration C (perfect graphane) are also indicated on the *x*-axis for comparison.

movement has given a substantial diffusion rate of ~8 s^{-1} for isolated H atoms at room temperature, 20 times of the value obtained by classical molecular dynamics method.[42] Indeed, small flux and long adsorption and diffusion time in our experiments resulted in better ordering than the opposite conditions. On the bottom side of graphene, the H atoms prefer to diffuse on the copper surface with a barrier of ~0.45 eV,[45] much faster than on graphene with a barrier of ~1 eV.[46] Then, the transfer of H atoms from the Cu surface to graphene becomes critical. Our climbing image nudged elastic band (NEB) simulations show that a topside-adsorbed H atom will greatly promote this process, lowering the transfer barrier from 1.21 eV (without the topside H) to 0.31 eV. This results in the preferential sticking configuration, the double-sided ortho-dimer. The H-assisted sticking process can go on and lead to the "growth" of the ordered configurations. We note that because the permeation barrier is prohibitively high for H to go through an intact graphene layer,[47] the intercalation needs to start at defect sites such as grain boundaries.[39,48] For this reason, suspended graphene may better facilitate the double-sided adsorption and similar H-assisted preferential sticking mechanisms should still work. Desorption and abstraction will affect the H saturation coverage.[7] Intertwined with adsorption and diffusion, they can have profound effects on ordering. Other factors including defects, surface curvature, and graphene–substrate interaction can further complicate the processes.[8,9] Systematic experimental and theoretical investigations of all these processes are much needed but beyond the scope of the current work. Nevertheless, our demonstration of the existence of ordered H configurations should inspire the design and synthesis of new ordered adsorbate structures to form new graphene-based functional materials.

Regarding magnetism, the three double-sided configurations are nonmagnetic because the magnetic moment induced by H adsorption is suppressed in the ortho-dimer unit. However, if we can keep the top-sided H atoms and remove the bottom-sided ones, the configurations become ferromagnetic because of the sublattice selectivity. Recent studies suggest that by using intense ultrashort p-polarized laser pulses with an asymmetric time envelope, selective removal of H atoms from one side of graphene can be achieved.[49]

In summary, ordered configurations of H adatoms on graphene were directly observed by STM. The H atoms in the configurations exhibit apparent sublattice selectivity and tiny deviations from the exact atop-of-carbon positions. STS measurements in regions containing the configurations showed a substantial gap in the LDOS as well as disorder-induced gap states. These findings can be well explained by our DFT simulations based on models of double-sided H configurations with disorder. Our results are relevant to band gap opening and obtaining specific magnetic orders in graphene.

■ ASSOCIATED CONTENT

Supporting Information

Additional information about the sample preparation, experimental methods and DFT calculations, and additional figures. This material is available free of charge via the Internet at http://pubs.acs.org.

■ AUTHOR INFORMATION

Corresponding Authors

*E-mail: (Y.F.) yexinfeng@pku.edu.cn.
*E-mail: (E.W.) egwang@pku.edu.cn.
*E-mail: (Z.H.) zhhu@pku.edu.cn.

Author Contributions

C.L., Y.F, and Y. X. contributed equally to this work.

Notes

The authors declare no competing financial interest.

■ ACKNOWLEDGMENTS

Z.H. and X.Z.L. thank the NBRP of China (Grants 2012CB921300 and 2013CB934600) and the Chinese Ministry of Education for financial supports. E.W., X.Z.L., and Z.H. thank the National Natural Science Foundation of China (Grants 11074005, 91021007, and 11275008) for financial supports.

■ REFERENCES

(1) Sofo, J. O.; Chaudhari, A. S.; Barber, G. D. *Phys. Rev. B* **2007**, *75* (15), 153401.
(2) Elias, D.; Nair, R.; Mohiuddin, T.; Morozov, S.; Blake, P.; Halsall, M.; Ferrari, A.; Boukhvalov, D.; Katsnelson, M.; Geim, A. *Science* **2009**, *323* (5914), 610–613.
(3) Ryu, S.; Han, M. Y.; Maultzsch, J.; Heinz, T. F.; Kim, P.; Steigerwald, M. L.; Brus, L. E. *Nano Lett.* **2008**, *8* (12), 4597–4602.
(4) Nair, R. R.; Ren, W.; Jalil, R.; Riaz, I.; Kravets, V. G.; Britnell, L.; Blake, P.; Schedin, F.; Mayorov, A. S.; Yuan, S. *Small* **2010**, *6* (24), 2877–2884.
(5) Schlapbach, L.; Züttel, A. *Nature* **2001**, *414* (6861), 353–358.
(6) Hornekær, L.; Baurichter, A.; Petrunin, V.; Field, D.; Luntz, A. *Science* **2003**, *302* (5652), 1943–1946.
(7) Ferro, Y.; Marinelli, F.; Allouche, A. *J. Chem. Phys.* **2002**, *116* (18), 8124–8131.

DOI: 10.1021/nl503635x
Nano Lett. 2015, 15, 903–908

(8) Balog, R.; Jørgensen, B.; Nilsson, L.; Andersen, M.; Rienks, E.; Bianchi, M.; Fanetti, M.; Lægsgaard, E.; Baraldi, A.; Lizzit, S. *Nat. Mater.* **2010**, *9* (4), 315−319.
(9) Grassi, R.; Low, T.; Lundstrom, M. *Nano Lett.* **2011**, *11* (11), 4574−4578.
(10) Haberer, D.; Vyalikh, D.; Taioli, S.; Dora, B.; Farjam, M.; Fink, J.; Marchenko, D.; Pichler, T.; Ziegler, K.; Simonucci, S. *Nano Lett.* **2010**, *10* (9), 3360−3366.
(11) Fiori, G.; Lebegue, S.; Betti, A.; Michetti, P.; Klintenberg, M.; Eriksson, O.; Iannaccone, G. *Phys. Rev. B* **2010**, *82* (15), 153404.
(12) Balakrishnan, J.; Koon, G. K. W.; Jaiswal, M.; Neto, A. C.; Özyilmaz, B. *Nat. Phys.* **2013**, *9* (5), 284−287.
(13) Yazyev, O. V. *Rep. Prog. Phys.* **2010**, *73* (5), 056501.
(14) Casolo, S.; Løvvik, O. M.; Martinazzo, R.; Tantardini, G. F. *J. Chem. Phys.* **2009**, *130* (5), 054704.
(15) Ferro, Y.; Teillet-Billy, D.; Rougeau, N.; Sidis, V.; Morisset, S.; Allouche, A. *Phys. Rev. B* **2008**, *78* (8), 085417.
(16) Novoselov, K.; Geim, A. K.; Morozov, S.; Jiang, D.; Katsnelson, M.; Grigorieva, I.; Dubonos, S.; Firsov, A. *Nature* **2005**, *438* (7065), 197−200.
(17) Zhang, Y.; Tan, Y.-W.; Stormer, H. L.; Kim, P. *Nature* **2005**, *438* (7065), 201−204.
(18) Skrypnyk, Y. V.; Loktev, V. M. *Phys. Rev. B* **2011**, *83* (8), 085421.
(19) Lebegue, S.; Klintenberg, M.; Eriksson, O.; Katsnelson, M. *Phys. Rev. B* **2009**, *79* (24), 245117.
(20) Flores, M. Z.; Autreto, P. A.; Legoas, S. B.; Galvao, D. S. *Nanotechnology* **2009**, *20* (46), 465704.
(21) Mirzadeh, M.; Farjam, M. *J. Phys.: Condens. Matter* **2012**, *24* (23), 235304.
(22) Pujari, B. S.; Gusarov, S.; Brett, M.; Kovalenko, A. *Phys. Rev. B* **2011**, *84* (4), 041402.
(23) Hornekær, L.; Šljivančanin, Ž.; Xu, W.; Otero, R.; Rauls, E.; Stensgaard, I.; Lægsgaard, E.; Hammer, B.; Besenbacher, F. *Phys. Rev. Lett.* **2006**, *96* (15), 156104.
(24) Hornekær, L.; Rauls, E.; Xu, W.; Šljivančanin, Ž.; Otero, R.; Stensgaard, I.; Lægsgaard, E.; Hammer, B.; Besenbacher, F. *Phys. Rev. Lett.* **2006**, *97* (18), 186102.
(25) Guisinger, N. P.; Rutter, G. M.; Crain, J. N.; First, P. N.; Stroscio, J. A. *Nano Lett.* **2009**, *9* (4), 1462−1466.
(26) Rougeau, N.; Teillet-Billy, D.; Sidis, V. *Chem. Phys. Lett.* **2006**, *431* (1), 135−138.
(27) Andree, A.; Lay, M. L.; Zecho, T.; Küpper, J. *Chem. Phys. Lett.* **2006**, *425* (1), 99−104.
(28) Lin, C.; Huang, X.; Ke, F.; Jin, C.; Tong, N.; Yin, X.; Gan, L.; Guo, X.; Zhao, R.; Yang, W.; Wang, E.; Hu, Z. *Phys. Rev. B* **2014**, *89* (8), 085416.
(29) Yin, X.; Li, Y.; Ke, F.; Lin, C.; Zhao, H.; Gan, L.; Luo, Z.; Zhao, R.; Heinz, T.; Hu, Z. *Nano Res.* **2014**, *7* (11), 1613−1622.
(30) Kresse, G.; Hafner, J. *Phys. Rev. B* **1993**, *47* (1), 558.
(31) Perdew, J. P.; Burke, K.; Ernzerhof, M. *Phys. Rev. Lett.* **1996**, *77* (18), 3865.
(32) Mills, G.; Jónsson, H.; Schenter, G. K. *Surf. Sci.* **1995**, *324* (2), 305−337.
(33) Cançado, L. G.; Jorio, A.; Ferreira, E. M.; Stavale, F.; Achete, C.; Capaz, R.; Moutinho, M.; Lombardo, A.; Kulmala, T.; Ferrari, A. *Nano Lett.* **2011**, *11* (8), 3190−3196.
(34) Ruffieux, P.; Gröning, O.; Schwaller, P.; Schlapbach, L.; Gröning, P. *Phys. Rev. Lett.* **2000**, *84* (21), 4910.
(35) Boukhvalov, D. *Physica E* **2010**, *43* (1), 199−201.
(36) Waqar, Z. *J. Mater. Sci.* **2007**, *42* (4), 1169−1176.
(37) Riedl, C.; Coletti, C.; Iwasaki, T.; Zakharov, A.; Starke, U. *Phys. Rev. Lett.* **2009**, *103* (24), 246804.
(38) Havu, P.; Ijäs, M.; Harju, A. *Phys. Rev. B* **2011**, *84* (20), 205423.
(39) Balgar, T.; Kim, H.; Hasselbrink, E. *J. Phys. Chem. Lett.* **2013**, *4* (12), 2094−2098.
(40) Dzhurakhalov, A. A.; Peeters, F. M. *Carbon* **2011**, *49* (10), 3258−3266.
(41) Šljivančanin, Ž.; Rauls, E.; Hornekær, L.; Xu, W.; Besenbacher, F.; Hammer, B. *J. Chem. Phys.* **2009**, *131* (8), 084706.
(42) Herrero, C. P.; Ramírez, R. *Phys. Rev. B* **2009**, *79* (11), 115429.
(43) Kerwin, J.; Jackson, B. *J. Chem. Phys.* **2008**, *128* (8), 084702.
(44) Aréou, E.; Cartry, G.; Layet, J.-M.; Angot, T. *J. Chem. Phys.* **2011**, *134* (1), 014701.
(45) Wang, X.; Fei, Y.; Zhu, X. *Chem. Phys. Lett.* **2009**, *481* (1), 58−61.
(46) Borodin, V.; Vehviläinen, T.; Ganchenkova, M.; Nieminen, R. *Phys. Rev. B* **2011**, *84* (7), 075486.
(47) Miao, M.; Nardelli, M. B.; Wang, Q.; Liu, Y. *Phys. Chem. Chem. Phys.* **2013**, *15* (38), 16132−16137.
(48) Tsetseris, L.; Pantelides, S. T. *J. Mater. Sci.* **2012**, *47* (21), 7571−7579.
(49) Zhang, H.; Miyamoto, Y.; Rubio, A. *Phys. Rev. B* **2012**, *85* (20), 201409.

DOI: 10.1021/nl503635x
Nano Lett. 2015, 15, 903−908